A CDMA based bidirectional communication system for hybrid fiber-coax CATV networks

A CDMA Based Bidirectional Communication System for Hybrid Fiber-Coax CATV Networks

Yvo L.C. de Jong, *Student Member, IEEE*, Robert P.C. Wolters, *Member, IEEE*, and Henrie P.A. van den Boom

Abstract— **Hybrid fiber-coax CATV networks are considered a promising infrastructure for the implementation of future interactive services. Efficient utilization of the available CATV spectrum requires a communication system which is dedicated to the specific properties of these networks. This paper presents the physical layer of a bidirectional communication system for HFC CATV networks which is based on CDMA, a technique that has a certain robustness to the ingress noise found in the CATV bandwidth. Because the application of asynchronous CDMA results in a poor spectral efficiency, a transmission scheme based on synchronous CDMA is adopted. Using synchronous CDMA and QPSK modulation, a capacity of 64 channels of 64 kbit/s each can be achieved in a bandwidth of 6 MHz. It is found that small synchronization errors can be tolerated without significant performance degradation. Next, a description is given of the cable modems responsible for the communication between subscribers and a CATV headend. The design exploits the typical CATV network configuration to enable a cost-effective hardware realization. Sensitivity of system performance to linear distortion is investigated by computer simulation. Especially linearly varying group delay and uneven amplitude response are shown to be potential causes of performance degradation.**

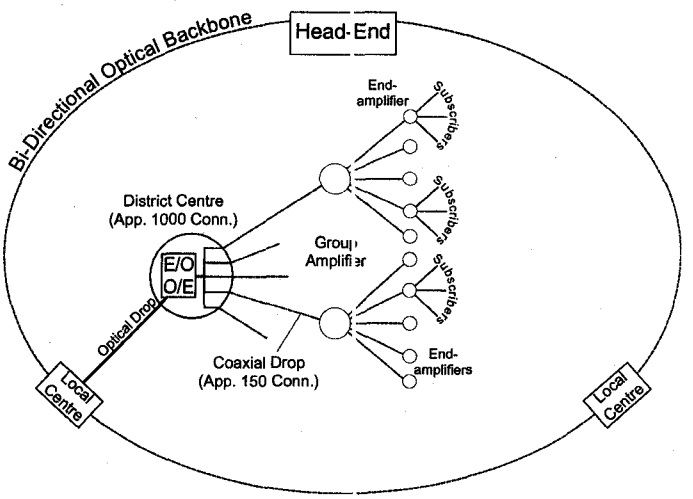

Fig. 1. Lay-out of a hybrid fiber-coax CATV network.

I. Introduction

LATELY, CATV networks are being considered not only as a reliable and cost-effective means to distribute analog audio and video signals to large groups of users, but also as a promising infrastructure for the implementation of new, interactive services. Especially the hybrid fiber-coax (HFC) network (view Fig. 1), in which relatively small coaxial access networks (typically 150 connections) are fed by separate optical fibers, is a suitable candidate for carrying broadband signals between a headend and individual subscribers. In recent years some CATV providers have equipped their networks with two-way actives, thus supporting bidirectional communications. In these networks a dedicated return bandwidth, which is separated from the downstream bandwidth by so-called diplex filters, is commonly reserved in the lower part of the CATV spectrum.

Due to noise funneling effects, this CATV upstream band is generally contaminated by high levels of both broadband and narrowband interference [1]. In particular, a number of severe narrowband interferers, which can be identified as shortwave radio broadcast signals coupled into the coaxial network parts, are found in the 5-15 MHz bandwidth region. Because the performance of existing FDMA and TDMA based communication systems is considerably degraded in the presence of narrowband interference, the lower part of the upstream spectrum is hardly used in practice. The use of a transmission method which is robust to narrowband noise would lead to a more efficient utilization of this band.

In this paper we present the physical layer of a bidirectional communication system which is dedicated to the specific properties of HFC CATV networks. The system design is based on the use of direct-sequence code division multiple-access (DS-CDMA), a transmission technique which shows a certain degree of resistance against narrowband interference and jamming. The transmission scheme is discussed in section II. In section III we give a description of the cable modems based on this scheme. In section IV, sensitivity of system performance to linear channel distortions is investigated by computer simulation. Finally, conclusions are drawn in section V.

II. Waveform selection

There has been increased interest in a transmission technique which is called direct-sequence code division

Y.L.C. de Jong and H.P.A. van den Boom are with the division of Telecommunications Technology and Electromagnetics (TTE), Eindhoven University of Technology (EUT), P.O. Box 513, 5600 MB Eindhoven, The Netherlands. Tel.: +31 40 247 3458/3444, fax: +31 40 2455197, e-mail: Y.L.C.d.Jong@ele.tue.nl/H.P.A.v.d.Boom@ele.tue.nl.

R.P.C. Wolters is now with Alcatel Telecom, Francis Wellesplein 1, B-2018 Antwerpen, Belgium. Tel.: +32 3 240 8472, fax: +32 3 240 9932, e-mail: WoltersR@btmaa.bel.alcatel.be.

Publisher Item Identifier: S 0018-9316(97)05618-7

multiple-access (DS-CDMA) [2], [3]. DS-CDMA is a multiple-access technique which is rather insensitive to the presence of narrowband interferers, due to its spread-spectrum properties. However, the most common form of DS-CDMA, in which there is no form of synchronization between the transmitters, provides poor spectral efficiency as compared to FDMA and TDMA. This low spectral efficiency, which is a result of the mutual interference between users, can be improved by applying signal processing techniques which are theoretically capable of reducing or even eliminating this interference [4]. In practice however, these so-called interference cancellation algorithms become too complex to be implementable for systems with a large number of users.

An alternative method to improve DS-CDMA capacity was proposed by De Gaudenzi [5] and requires the very accurate synchronization of simultaneous transmissions. This allows the use of (quasi-)orthogonal spreading sequences, which results in (almost) no interference between users. Synchronous DS-CDMA (S-CDMA) is expected to be a very appropriate transmission scheme for application in the HFC network, because its fixed configuration enables accurate synchronization of transmissions. In the downstream link this synchronization is straightforward, because all transmitters are situated at the same location (the headend). In the upstream link the transmitters experience various transmission delays in the paths to the headend. However, synchronization of upstream signals is automatically maintained once it has been established.

A. Modulation

Much effort has been done to investigate the achievable capacity of communication systems based on asynchronous DS-CDMA (A-CDMA). Results in [6] show that the use of high-order modulation techniques does not necessarily improve the A-CDMA capacity, due to the fact that such a method would exhibit more vulnerability to the background noise and interference, while it would only increase multiple-access interference (MAI). Under practical circumstances, the performance of QPSK is shown to be slightly better than that of BPSK, and much better than that of 16-QAM.

In contrast with A-CDMA, S-CDMA provides good channel separation due to the encoding of the transmissions with (almost) orthogonal spreading sequences. Therefore, S-CDMA provides the possibility to employ higher-order modulation. This reduces the bandwidth of the data modulated carrier before spreading, thus allowing the use of longer spreading sequences. Because in general the number of available sequences is proportional to the sequence length, this leads to improved user capacity.

Consider an S-CDMA communication system with data bit rate R_b and N_u active users, employing M-ary QAM modulation and a processing gain G_p. The error performance of this S-QAM-CDMA system can be obtained as follows. If for a given system bandwidth a BPSK modulated S-CDMA system can employ spreading sequences of length G_p, a system based on M-ary QAM, in which $m = \log_2 M$ bits are represented by one symbol, can utilize sequences of length mG_p. Assuming perfect synchronization and power control, and an ideal channel, the signal at the input of the receiver is

$$r(t) = A\sum_{i=1}^{N_u} d_i^i(t)c_i^i(t)\cos(\omega_c t + \theta_i) + \\ + A\sum_{i=1}^{N_u} d_i^q(t)c_i^q(t)\sin(\omega_c t + \theta_i) + n(t), \tag{1}$$

with

$$d_i^i(t) = \sum_{k=-\infty}^{+\infty} d_{2k,i}p_T(t - kT) \tag{2}$$

and

$$d_i^q(t) = \sum_{k=-\infty}^{+\infty} d_{2k-1,i}p_T(t - kT) \tag{3}$$

the information-bearing waveforms in the in-phase (I) and quadrature (Q) channels, respectively, and

$$c_i^{i/q}(t) = \sum_{k=-\infty}^{+\infty}\sum_{l=0}^{mG_p-1} c_{l,i}^{i/q}p_T(t - lT_c - kT) \tag{4}$$

the corresponding spreading waveforms. The elements of the data sequence $d_{k,i}$ can take on the values $\pm(2l+1)$, $l = 0, 1, \ldots, (m-1)/2$, and the elements of the spreading sequences $c_{l,i}^{i/q}$ take on the values ± 1. In equation (1), A, ω_c and θ_i are the amplitude, the carrier frequency, and the carrier phase of the ith user, respectively; $n(t)$ is the channel noise process with average two-sided power spectral density $N_0/2$, $T = mG_pT_c$ is the symbol period, $T_c = R_c^{-1}$ is the chip period, and $p_T(t)$ is a unit-amplitude rectangular pulse waveform which is zero for $t < 0$ and $t > T$.

The jth receiver consists of a pair of synchronized correlation receivers (view Fig. 2), one of them matched to the I and the other to the Q channel. For the determination of the average bit error probability, only the SNR at the output of the I correlator will be evaluated. By symmetry, the SNR in the Q branch will be the same. The output of the in-phase correlator of the jth receiver is

$$y_j^i = \frac{AT}{2}d_{0,j} + \psi + \eta, \tag{5}$$

where ψ is the multiple-access interference (MAI), and η is a zero-mean Gaussian noise term with variance $\sigma_\eta^2 = N_0T/4$. In the derivation of (5), the double frequency components of $r(t)\cos(\omega_c t + \theta_j)$ have been neglected.

The variance of the MAI can be written as

$$\sigma_\psi^2 = \frac{A^2T^2}{8m^2G_p^2}\sum_{i=1,i\neq j}^{N_u} E\{d_{0,i}^2\}\left[\sum_{l=0}^{mG_p-1} c_{l,i}^i c_{l,j}^i\right]^2 \\ + \frac{A^2T^2}{8m^2G_p^2}\sum_{i=1,i\neq j}^{N_u} E\{d_{-1,i}^2\}\left[\sum_{l=0}^{mG_p-1} c_{l,i}^q c_{l,j}^i\right]^2. \tag{6}$$

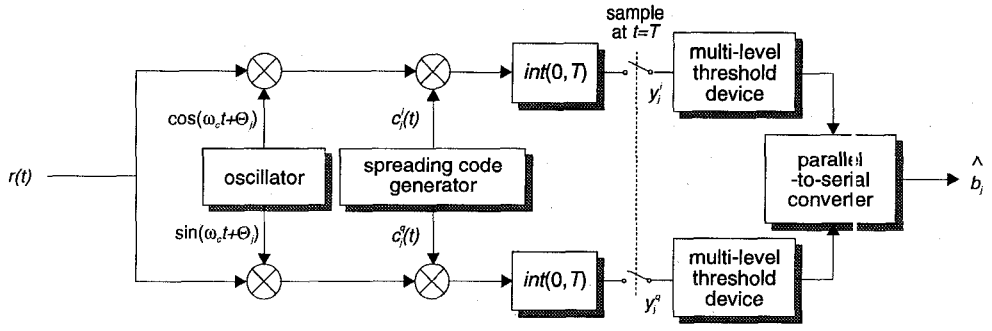

Fig. 2. Simplified model of an S-QAM-CDMA receiver.

The expectances $E\{d_{0,i}^2\}$ and $E\{d_{-1,i}^2\}$ can be shown to equal $(2^m-1)/3$ [7], and (6) reduces to

$$\sigma_\psi^2 = \frac{A^2T^2(2^m-1)}{24m^2G_p^2}(N_u-1)(\mu_j^i+\mu_j^q), \tag{7}$$

where

$$\mu_j^{i/q} = \frac{1}{N_u-1}\sum_{i=1,i\neq j}^{N_u}\left[\sum_{l=0}^{mG_p-1} c_{l,i}^{i/q}c_{l,j}^{i}\right]^2 \tag{8}$$

are the quadratic average I/Q cross-correlation factors for the jth user [5]. Usually, these factors $\mu_i^{i/q}$ are equal for all users i $(1 \le i \le N_u)$ and for the I and Q channels, say μ.

If the QAM signal constellation is assigned a perfect 2-dimensional Gray code [7], the probability of bit error can now be approximated by

$$P_b = 4\left(\frac{\sqrt{2^m}-1}{m\sqrt{2^m}}\right) \times Q\left(\sqrt{\frac{3mE_b/(2^m-1)}{N_0+(\mu/mG_p^2)(N_u-1)E_b}}\right), \tag{9}$$

which is valid for high SNR. In this equation, $E_b = A^2T(2^m-1)/3m$ is the bit energy per user.

B. Spreading sequences

For a given processing gain $G_p = R_c/R_b$, where the chip rate R_c is limited by the available system bandwidth, the average BER as a function of the bit SNR E_b/N_0 is given by (9) for QAM modulation. Here, the quadratic cross-correlation factor μ represents the effect of the applied spreading sequences on the system performance. Obviously, for a perfectly synchronized DS-CDMA system utilizing orthogonal codes, $\mu = 0$. In this case, (9) reduces to the well-known expression for the bit error probability of M-ary QAM in conventional digital communications.

In the CATV return link, it may not be possible to maintain perfect chip synchronization. Assuming that there will be small errors in synchronization, orthogonal sequences with small cross-correlation for small synchronization offsets should be used. Work in [8] suggests that orthogonal sequences based on the Sylvester-type Hadamard matrices (Walsh codes) are optimum for synchronization errors smaller than one chip period However, a serious disadvantage of the application of Walsh codes is that it requires external network synchronization in the return link. Walsh codes have poor out-of-phase cross-correlation properties since they are optimized with respect to zero-phase only. As a result, the upstream transmissions of subscribers who are connecting to the network but are not in synchronization yet would severely interfere with the synchronous transmissions. An S-CDMA system using a separate timing channel would not fully exploit the advantages of CDMA and could result in a more complex hardware realization.

In [5], a set of CDMA codes was proposed which are almost orthogonal at zero-phase and in addition have pseudo-noise properties. These so-called preferentially-phased Gold sequences can be applied asynchronously for synchronization purposes at the cost of almost no performance loss in synchronous use, as compared to orthogonal sequences. For a sequence length of N, the number of preferentially-phased Gold sequences amounts to $N+1$. Their quadratic average cross-correlation factor is $\mu = 1$ for all possible sequence lengths. Preferentially-phased Gold sequences are optimum in the sense that there exist no larger sets of sequences having this correlation property. Based on the above observations, preferentially-phased Gold sequences were selected for application in the CATV communication system.

Plots of the error performance of S-CDMA using preferentially-phased Gold codes are given in Fig. 3 for $M = 4$, $M = 16$ and $M = 64$. The error performance of S-CDMA using BPSK is given for comparison. The results in Fig. 3 have been computed using (9), which implies that perfect synchronization and power control are assumed. For BPSK and QPSK, the error performance is seen to be hardly dependent on the number of simultaneous users. However, 16-QAM and 64-QAM show increased sensitivity to MAI. For application in the CATV network, the higher capacity that can be achieved using 16-QAM or higher-order modulation formats is offset by the relatively high required bit SNR and the hardware complexity. On the other hand, the use of QPSK doubles capacity as compared with binary PSK, at virtually no loss of error performance. Furthermore, QPSK is known as a simple and reliable modulation technique. QPSK was therefore selected as the modulation scheme.

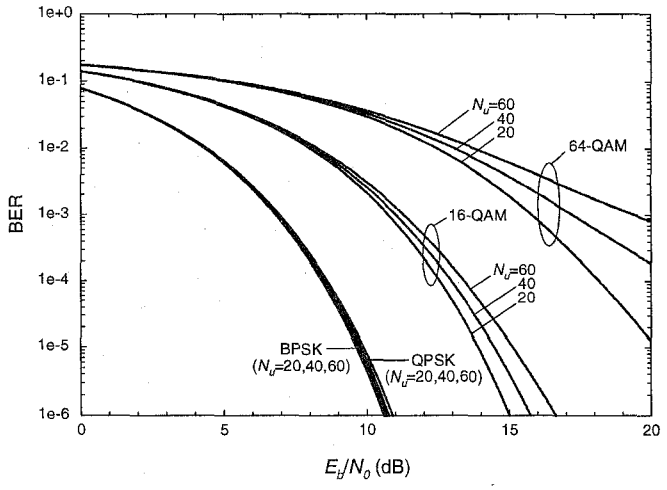

Fig. 3. Error performance of S-CDMA using different modulation formats. The processing gain G_p=18 dB. N_u is the number of active users.

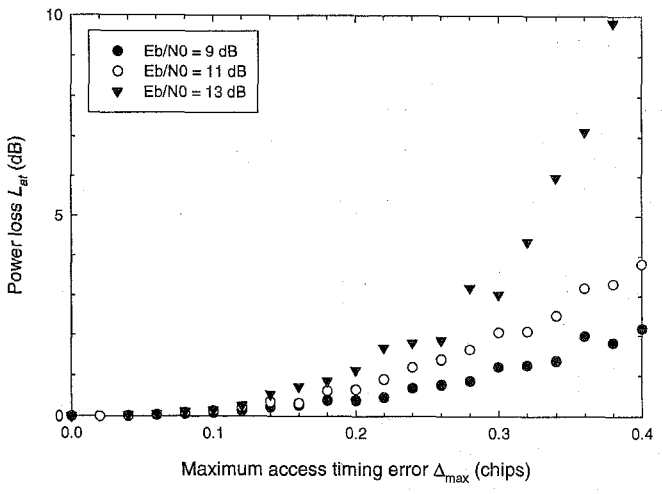

Fig. 4. Sensitivity of S-QPSK-CDMA to synchronization errors, for a BER of 10^{-4} and for different values of the bit SNR E_b/N_0. The processing gain $G_p = 18$ dB, and the number of active users $N_u = 64$.

Using independent preferentially-phased Gold sequences for the I and Q channels, a capacity of 64 channels of 64 kbit/s each can be achieved in a bandwidth of 6 MHz, which is approximately the bandwidth occupied by an analog television channel. The choice for a 6 MHz system bandwidth enables a flexible assignment of bandwidth within the CATV spectrum.

C. Effects of imperfect synchronization and power control

The performance of a perfectly synchronized S-QPSK-CDMA system depends on the cross-correlation of the applied code sequences at zero-phase only. However, small access timing errors may result in a degradation of the error performance. Furthermore, imperfect power control may cause increased interference between users, again leading to performance degradation. Therefore, computer simulations were carried out to estimate how the S-QPSK-CDMA system performance is affected by imperfect synchronization and power control. In these simulations, the quantity of interest is the excess signal power needed to maintain the desired BER. We will refer to this quantity as the power loss L.

Fig. 4 shows the power loss due to access timing errors (L_{at}) as a function of the maximum access timing error $\Delta_{\max}$, for a BER of 10^{-4} and different values of E_b/N_0. The distribution of the access timing errors is assumed to be uniform in the interval $(-\Delta_{\max}, +\Delta_{\max})$. It is observed that L_{at} becomes unacceptably large for synchronization errors greater than ca. $0.3{\cdot}T_c$. A maximum synchronization error of $T_c/8$ however results in negligible power loss (< 0.3 dB) and was taken as a design objective.

The power loss as a function of the maximum power control error $\Delta P_{\max}$ (L_{pc}) is plotted in Fig. 5, for a BER of 10^{-4} and different values of E_b/N_0. The distribution of the power level deviations is assumed to be uniform in the interval $(-\Delta P_{\max}, +\Delta P_{\max})$, $\Delta P_{\max}$ in dB. These results show almost no sensitivity of system BER to imperfect power control.

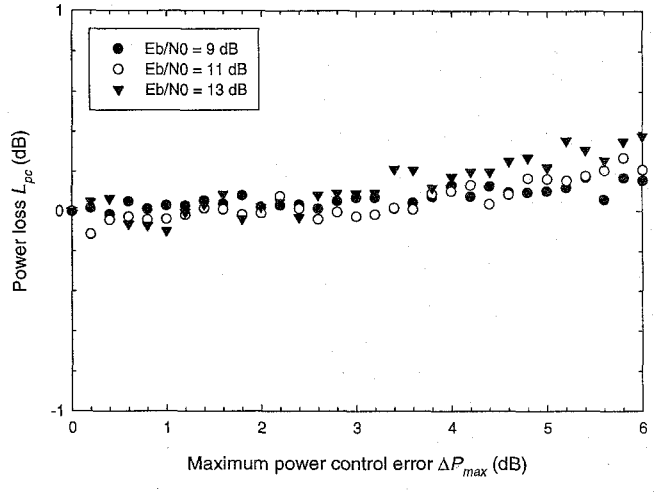

Fig. 5. Sensitivity of S-QPSK-CDMA to imperfect power control, for a BER of 10^{-4} and for different values of the bit SNR E_b/N_0. The processing gain $G_p = 18$ dB, the number of active users $N_u = 64$, and the maximum synchronization error $\Delta_{\max} = T_c/8$.

III. The Cable Modem

A. Transmitter

The basic building blocks of the downstream and upstream transmitter are shown in Fig. 6. The functionality of both transmitters is essentially the same. The input data stream is differentially encoded and split into an I and a Q stream, both at half the bit rate. These I-Q symbol streams are then spread by independent preferentially-phased Gold sequences. After pulse shaping by a square-root raised cosine transmit filter with $x/\sin x$ aperture equalization, the spread baseband signal is D/A converted and modulated on the I-Q carrier components generated by an oscillator.

The configuration of the downstream transmitters ex-

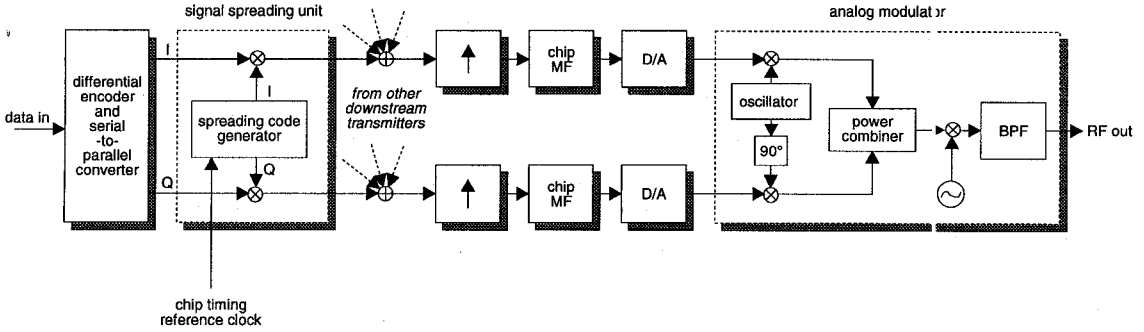

(a) downstream

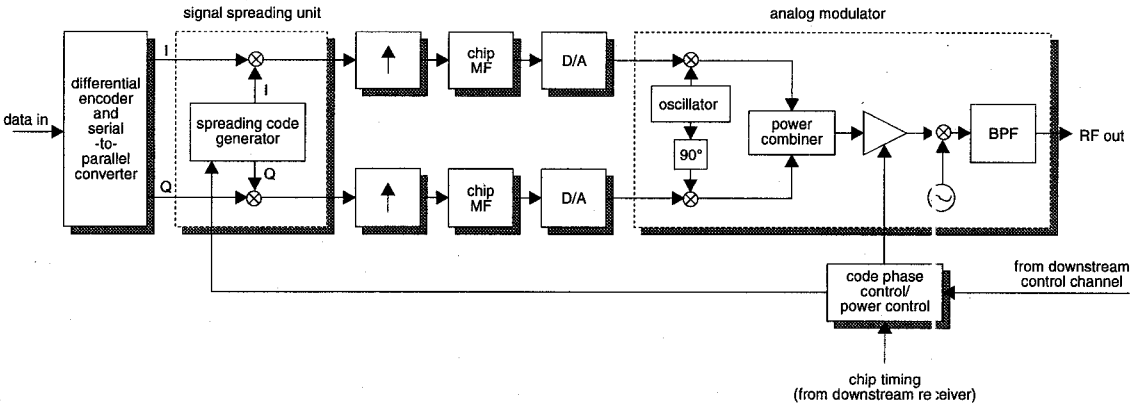

(b) upstream

Fig. 6. Block diagrams of transmitters in an S-QPSK-CDMA system.

ploits the fact that they are all at the same physical location (the headend). Because the chip timing of all downstream transmitters is controlled by a common chip timing reference clock, the downstream transmissions are automatically synchronized. Furthermore, because the spread signals are summed in the digital domain before analog modulation, a single carrier can be used for all downstream signals. This solution facilitates carrier recovery and coherent detection at the downstream receivers.

Upstream transmissions are synchronized by means of feedback of chip timing information from the headend receiver to each individual upstream transmitter via a downstream control channel. At initial connection to the network, each subscriber modem transmits asynchronous preferentially-phased Gold sequences to the headend receiver. The proper chip clock frequency is derived from the received downstream transmissions. The correct code phase is found during a procedure in which the subscriber modem shifts the phase of its transmitted code sequences until it is notified by the headend modem that synchronization has been acquired. During the same procedure, the transmitted power is adjusted to the desired level. Since the transmission paths in the CATV network are fixed, no further code phase re-acquisition or power control has to be performed after the initial connection to the network. The transmission of unsynchronized spreading sequences results in a relatively high level of MAI, which degrades the system BER. The number of asynchronous users attempting to connect to the network must therefore be limited by the connectivity protocol. These are aspects which are currently under investigation.

B. Receiver

Fig. 7 depicts the basic building blocks of the downstream and upstream receiver. Coherent detection of the downstream information is performed after recovery of the common carrier frequency and phase using an analog phase locked-loop. On the other hand, coherent detection of the upstream information is not that simple, because the received carriers have independent frequency and phase. Therefore, carrier recovery cannot take place prior to signal despreading. In the upstream receiver in Fig. 7 we employ a local oscillator which is not controlled by a carrier recovery circuit, but has a frequency close to those of the received carriers. Removal of the residual modulation is realized in the digital domain by a digital phase-locked loop (DPLL). Using this approach, a single analog demodulator subsystem can be shared by all upstream receivers. Besides this analog circuit, the upstream receivers also share the A/D converters, chip matched filters and interpolation

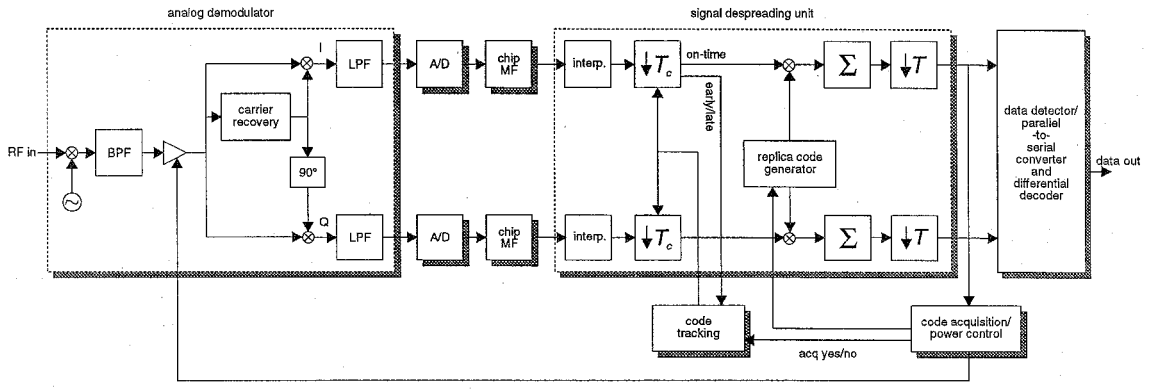

(a) downstream

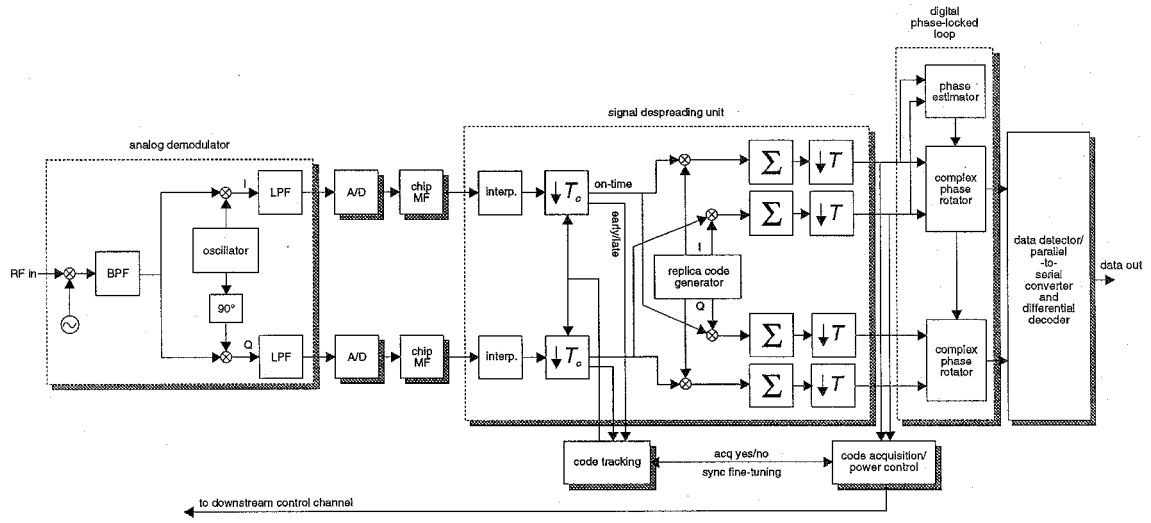

(b) upstream

Fig. 7. Block diagrams of receivers in an S-QPSK-CDMA system.

filters, to reduce costs per user.

At the upstream receiver, the unknown carrier phase of the received signal is recovered by a digital carrier recovery subsystem, as shown in Fig. 8. In addition to resolving a fixed carrier phase, this circuit must be able to track linearly increasing or decreasing carrier phase resulting from local oscillator frequency offsets relative to the received carrier frequency. The subsystem consists of a complex phase rotator controlled by a phase estimator, which provides an estimation of the received carrier phase. This estimation is based on an error signal which is in turn provided by the complex phase rotator.

The remaining receiver functionality is in principle the same for the downstream and upstream receiver. The baseband I-Q signals are sampled asynchronously and subsequently filtered. Then they are down-sampled to chip rate synchronously with the chip timing that is recovered by a so-called early-late correlator which is described and analyzed in detail in [9]. It should be noted that this scheme works properly only if the received code phase has already

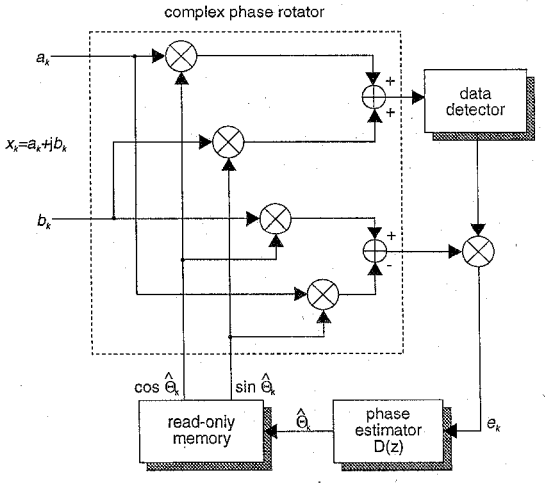

Fig. 8. Block diagram of the digital carrier recovery subsystem.

been synchronized with the replica code to within $\pm T_c/2$. This coarse code alignment is performed by the code acquisition subsystem in the initial synchronization procedure, before the actual data transfer takes place. The chip streams produced by the chip timing recovery subsystem are despread by means of multiplication with the I-Q replica code sequences and subsequent accumulation over the sequence length. The resulting samples at symbol rate are used for data extraction. Differential decoding is performed to remove phase ambiguity from the detected data sequence.

IV. Simulation of linear distortion effects

Because of the narrow guard band between the upstream and the downstream CATV spectrum, the diplex filters in the path between subscribers and the headend inevitably introduce linear channel distortion in the passbands. The larger the number of cascaded two-way actives, the more distortion will be experienced. This number is only two in modern HFC networks, but may be much higher in more conventional networks. Computer simulations were performed to assess the effects of linear distortion on the modem performance in the upstream link. A simulation model based on quasi-analytic BER estimation [10] was used, in which the relevant signal and noise parameters at the input of the receiver threshold device are determined by simulation, and a BER estimation is then made with a formula.

A. Transmitter model

The user data is generated using the output of a pseudo-random number generator. Subsequent vectors of 127 preferentially-phased Gold sequence elements are multiplied by the corresponding data bits. The resulting chip sequences drive impulse generators, which produce zeros and one unit magnitude impulse per 32 output samples. Each pair of impulse streams corresponding to a single user is shifted in time randomly by -4 to +4 samples, corresponding to a maximum synchronization error of $T_c/8$ with respect to the first user, whose signal is shifted by zero samples. The time-shifted user signals are shaped by a 511-tap digital square-root raised cosine transmit filter with roll-off factor $\alpha = 0.4$, and decimated to four samples per chip. Finally, each pair of I and Q signals is converted up in frequency by multiplication with orthogonal carriers with a frequency close to that of the local oscillator at the receiver, and with random phase. The sum of all CDMA signals is fed to the channel.

B. Channel model

Both the amplitude and the group delay characteristics of the upstream CATV channel can be approximated by a combination of linear and sinusoidal frequency dependence. To simulate the effects of these forms of channel distortion individually, digital filters were designed with either constant group delay and prescribed amplitude response, or with constant amplitude response and prescribed group delay. Finite impulse response (FIR) filters with symmetrical coefficients were used in the first case, while we adopted a somewhat more complicated design procedure [11] for the second case.

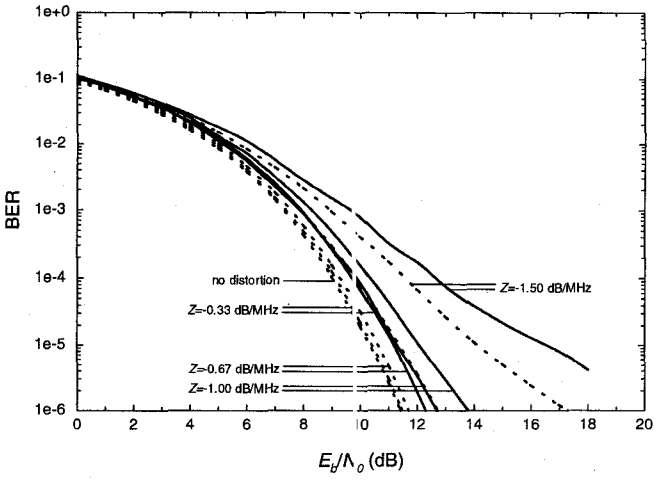

Fig. 9. System BER versus E_b/N_0 for perfect (dashed) and imperfect (solid) chip timing and carrier recovery subsystems in a channel with linear amplitude distortion

C. Receiver model

At the receiver input, a Gaussian noise signal is added, and baseband conversion is performed by multiplication with orthogonal carriers. In the simulations, only local oscillator frequency offsets smaller than 500 Hz have been considered. This is a realistic figure, since commercially available quartz crystal oscillators are accurate with respect to their nominal frequency to within a few ppm. The resulting baseband signal, which has still unrecovered carrier phase, is further processed by the digital part of the receiver. At the input of the decision threshold devices, the average signal power is computed, as well as the variance of the accompanying noise. Under the Gaussian assumption, the predicted system BER is calculated by applying the Gaussian probability function to the ratio of the average signal power to the rms noise power specified at the detector input.

D. Results

Linear amplitude distortion

Simulation results are shown in Fig. 9 for linear amplitude distortion of the form $A(f) = Z \cdot f$. Results are given for both the case of perfect (dashed) and imperfect (solid) timing and carrier recovery. The constant Z is varied from 0 to -1.50 dB/MHz, where $Z = 0$ corresponds to the case with no distortion. The degradation for values of Z better than -0.67 dB/MHz is seen to be small: less than 0.4 dB. Degradation due to imperfect subsystems is smaller than 1 dB for these values of Z. For $Z = -1.00$ dB/MHz and $Z = -1.50$ dB/MHz, the error performance deterioration is clearly more serious. For $Z = -1.50$ dB/MHz, degradation due to imperfect timing and carrier recovery is on the order of 1 dB at a BER of 10^{-4}.

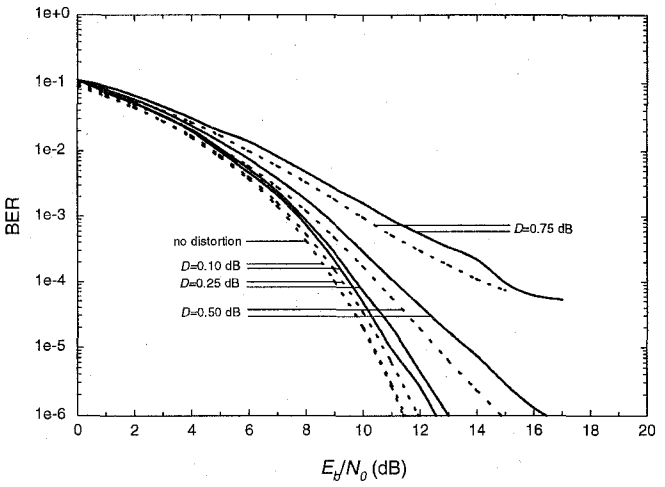

Fig. 10. System BER versus E_b/N_0 for perfect (dashed) and imperfect (solid) chip timing and carrier recovery subsystems in a channel with sinusoidal amplitude distortion.

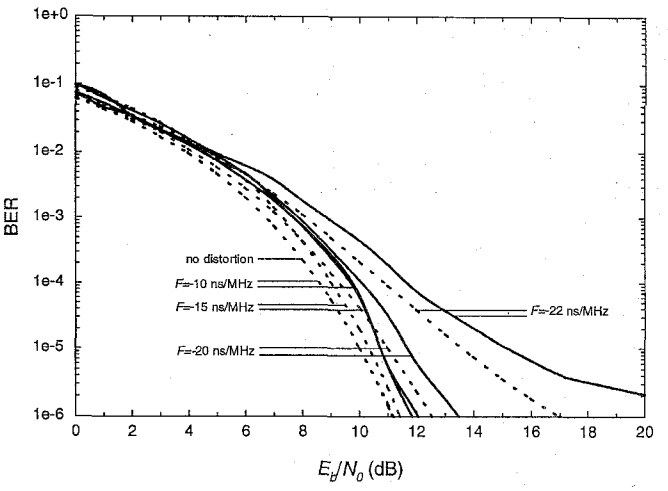

Fig. 11. System BER versus E_b/N_0 for perfect (dashed) and imperfect (solid) chip timing and carrier recovery subsystems in a channel with linear group delay distortion.

Sinusoidal amplitude distortion

For the case of sinusoidal amplitude distortion, i.e. an amplitude characteristic of the form $A(f) = -D \cdot \cos(15\pi f/f_r)$, $f_r = 8.128$ MHz, simulation results are presented in Fig. 10. The amplitude D is varied from 0 to 0.75 dB, where $D = 0$ corresponds to the ideal channel. Again, results are shown both for perfect (dashed) and imperfect (solid) timing and carrier recovery. Performance loss is seen to be small (< 0.5 dB) for values of D smaller than 0.25 dB. Furthermore, degradation due to non-ideal timing and carrier tracking is smaller than 1.6 dB for all considered values of D. At a BER of 10^{-4}, sinusoidal amplitude distortion causes a decrease in performance of 1.5 dB for $D = 0.50$ dB and of 5.5 dB for $D = 0.75$ dB.

Linear group delay distortion

Fig. 11 shows simulation results for linear group delay distortion of the form $t_g(f) = F \cdot f$. The slope F is varied from 0 to -22 ns/MHz. For values of F better than -15 ns/MHz, system performance is found to be degraded less than 0.5 dB when there is assumed to be perfect timing and carrier recovery. However, imperfect subsystems cause a decrease in performance of more than 1 dB at a BER of 10^{-4}. For values of F worse than -20 ns/MHz, system performance deteriorates rapidly.

Sinusoidal group delay distortion

The simulated effects of sinusoidal group delay distortion of the form $t_g(f) = -C \cdot \cos(16\pi f/f_r)$, $f_r = 8.128$ MHz, are depicted in Fig. 12. The amplitude C takes on the values 0 to 200 ns. Performance loss is found to be small (< 0.5 dB) for amplitudes smaller than 100 ns, when there is ideal timing and carrier tracking. For $C = 200$ ns, degradation is still on the order of only 1.2 dB. However, imperfect subsystems cause extra performance degradation of ca. 1 dB at a BER of 10^{-4}.

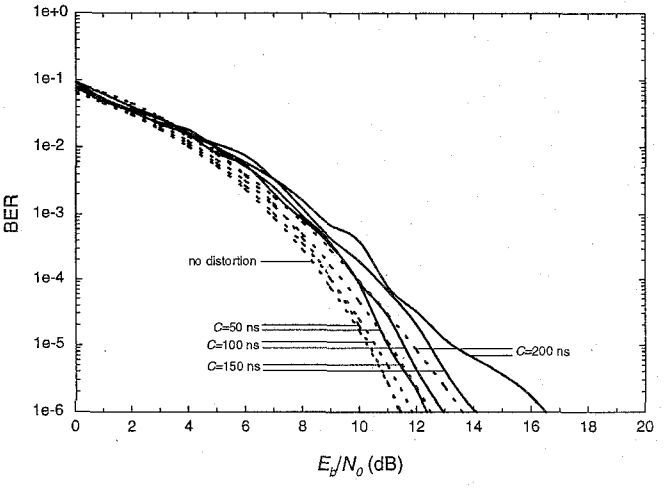

Fig. 12. System BER versus E_b/N_0 for perfect (dashed) and imperfect (solid) chip timing and carrier recovery subsystems in a channel with sinusoidal group delay distortion.

From the above figures, it may be concluded that the degradation of E_b/N_0 as a function of the total amplitude variation in the 6 MHz system bandwidth is much higher for sinusoidal than for linear amplitude distortion. In contrast, the degradation as a function of the total group delay variation in the system bandwidth is higher for linear than for sinusoidal group delay distortion. We therefore expect that in particular a linearly varying group delay and uneven amplitude response are serious potential causes of degradation. In modern HFC networks, performance loss due to linear distortion will be very limited. In less modern networks with large numbers of cascaded amplifiers however, channel equalization techniques might be required.

V. Conclusions

In this paper, we have presented a bidirectional 64 kbit/s communication system which is dedicated to the specific

properties of HFC CATV networks. The system is based on DS-CDMA, because this multiple-access technique has inherent robustness to the narrowband noise which is found in especially the 5-15 MHz frequency region of the upstream channel. However, because CDMA is typically a complex technique, its application might be less favorable in the downstream channel, where simpler access techniques can be utilized.

Some specific CATV network properties have been exploited in order to achieve a cost-effective and bandwidth-efficient design. Firstly, because all downstream transmitters and upstream receivers are concentrated at the headend, a considerable amount of hardware can be shared by all modems. Also, this enables the accurate synchronization of downstream transmissions required using synchronous, high-capacity CDMA. Finally, since the CATV network topology is fixed, it is expected that upstream transmissions can also be synchronized in a rather simple way.

The performance of the upstream receiver in the presence of linear channel distortion has been investigated using a simulation model. It was found that in particular a linear group delay and an uneven amplitude response are potentially harmful. Yet, in modern HFC networks linear distortion is expected to result in only very limited system performance degradation.

At this time, prototypes of the CDMA modems are under development. Preparations are being made to conduct field trials in an operational network.

Acknowledgment

The authors would like to thank the Dutch Technology Foundation (STW) for the financial support of this project.

References

[1] R.P.C. Wolters, "Characteristics of Upstream Channel Noise in CATV-Networks," accepted for publication in IEEE Transactions on Broadcasting.

[2] R.C. Dixon, *Spread Spectrum Systems with Applications*, John Wiley and Sons, Inc., 1994.

[3] R.E. Ziemer and R.L. Peterson, *Digital Communications and Spread Spectrum*, MacMillan Publishing, New York, 1985.

[4] S.G. Glisic and P.A. Leppanen (Eds.), *Code Division Multiple Access Communications*, Kluwer, Dordrecht, The Netherlands, 1995.

[5] R. De Gaudenzi and C. Elia, "Bandlimited Quasi-Synchronous CDMA: A Novel Satellite Access Technique for Mobile and Personal Communication Systems," *IEEE Journal on Selected Areas in Communications*, vol. 10, no. 2, pp. 328–343, Feb. 1992.

[6] R.L. Pickholtz *et al*, "Optimization of the Processing Gain of an M-ary Direct-Sequence Spread Spectrum Communication System," *IEEE Transactions on Communications*, vol. 8, pp. 1389–1398, Aug. 1980.

[7] M.K. Simon, S.M. Hinedi, and W.C. Lindsey, *Digital Communication Techniques*, Prentice Hall, 1990.

[8] V.M. DaSilva and E.S. Sousa, "Multicarrier Orthogonal CDMA Signals for Quasi-Synchronous Communication Systems," *IEEE Journal on Selected Areas in Communications*, vol. 5, no. 5, pp. 842–852, June 1994.

[9] R. De Gaudenzi, M. Luise, and R. Viola, "Chip Timing Synchronization in an All-Digital Band-Limited DS/SS Modem," in *Proceedings of the International Conference on Communications 1991 (ICC'91)*, 1991, pp. 1688–1692.

[10] M.C. Jeruchim, P. Balaban, and K.S. Shanmugan, *Simulation of Communication Systems*, McGraw-Hill, New York, 1968.

[11] H.W. Schuessler and P. Steffen, "On the Design of Allpasses with Prescribed Group Delay," in *Proceedings of the International Conference on Acoustics, Speech and Signal Processing (ICASSP90)*, New York, 1990 vol. 3, pp. 1313–1316.